Efficient Extraction of Neutral Heterocyclic Nitrogen Compounds from Coal Tar *via* Ionic Liquids and Its Mechanism Analysis

Lianzheng Zhang [a], Mi Zhang [a], Jun Gao [a], Dongmei Xu* [a], Shixue Zhou [a], Yinglong Wang [b]*

[a] College of Chemical and Environmental Engineering, Shandong University of Science and Technology, Qingdao 266590, China

[b] College of Chemical and Engineering, Qingdao University of Science and Technology, Qingdao 266042, China

*Corresponding author

Jun Gao, E-mail address: gao@sdust.edu.cn, Tel: +86-532-86057103

Dongmei Xu, E-mail address: xudongmei.cn@163.com, Tel: +86-532-86057798

Part 1 The typical aromatic compositions of coal tar

Table S1. The typical aromatic compositions of coal tar.

Type	1 ring	2 rings	3 rings	4 rings
Aromatic	Benzene, toluene, xylene, biphenyl	Indene [1], naphthalene [1], methylnaphthalene [1] and its homologues, tetrahydronaphthalene	Fluorene [1], acenaphthene, acenaphthylene [1], anthracene [1], phenanthrene [1]	Perylene [1], chrysene, fluoranthene [1]
Oxygenate compounds	Phenols, furans, diphenyl ethers	Benzofuran, naphthol	Dibenzofuran [1], anthralin, phenanthrol	Complex polycyclic phenol
Nitrogen compounds	Thiophenol, thiophene, disulfide	Thianaphthene, naphthalenethiol	Dibenzothiophen,	Complex polysulfophenol
Sulfur compounds	Pyridines, azoles, benzonitrile	Indole, quinoline, isoquinoline	Carbazole [1], acridine, phenanthridine	Complex nitrogen heterocycle

[1] The mass compositions ≥1% in coal tar.

Part 2 Appropriate IL extractants' selection by COSMO-SAC model

The COSMO-SAC model, derived from the conductor-like screening model (COSMO), was first proposed by Lin and Sandler [1] and used to predict the activity coefficients in solutions. In the recent published literatures, the COSMO-SAC model has been applied in phase equilibrium prediction, solubility calculation and solvent screening, etc. [2-4]. The COSMO-SAC model calculation consists of two steps, viz, the quantum chemical calculation to generate the COSMO file and the calculation of the activity coefficient from the COSMO file. The details of the COSMO-SAC model can be found in the previous publications [5, 6] and our previous works [7, 8]. The detailed structures of the cations and anions used in this work are listed in Table S2.

Table S2. The structures and names of the anions and cations.

Number	Name	Abbreviation	Structural
		Anions	
1	Chloride	Cl^-	
2	Brimide	Br^-	
3	Iodine	I^-	
4	Acetate	Ac^-	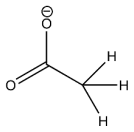
5	Propionate	Pro^-	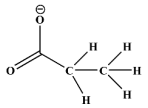
6	Trifluoroacetate	TFA^-	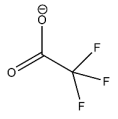
7	Tosylate	TOS^-	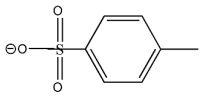
8	Trifluoromethanesulfonate	OTf^-	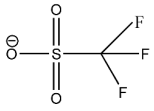

9	Methyl sulfate	$MeSO_4^-$	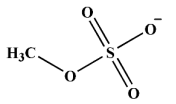
10	Ethyl sulfate	$EtSO_4^-$	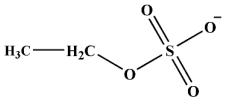
11	Methoxyethyl sulfate	$CH_3OEtSO_4^-$	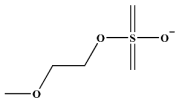
12	Perfluorobutanesulfonate	$PFBS^-$	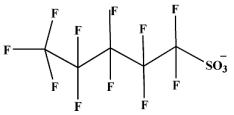
13	Hydrogen sulfate	HSO_4^-	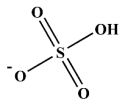
14	Dihydrogen phosphate	$H_2PO_4^-$	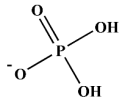
15	Dimethylphosphate	$Me_2PO_4^-$	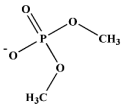
16	Perfluorophosphate	FAP^-	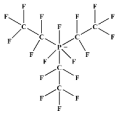
17	Hexafluorophosphate	PF_6^-	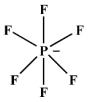
18	Tetrafluoroborate	BF_4^-	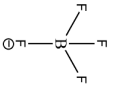
19	Boron cyanide	TCB^-	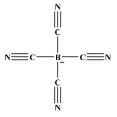
20	Hexafluoroantimonate	SbF_6^-	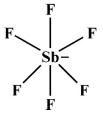
21	Perchlorate	ClO_4^-	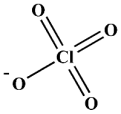
22	Nitrate	NO_3^-	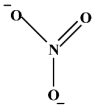
23		$AlCl_4^-$	**$AlCl_4^-$**
24		$FeCl_4^-$	**$FeCl_4^-$**

25	Thiocyanate	SCN^-	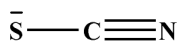
26	Tricyanomethane	TCM^-	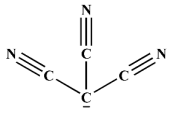
27	Dicyanamide	DCA^-	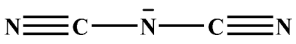
28	Bis((trifluoromethyl) sulfonyl) imide	NTf_2	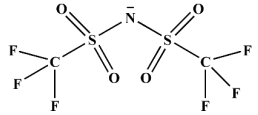
29	Phenoxy group	PhO^-	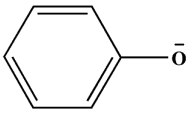
	Cations		
1	1-Ethyl-3-methylimidazoliu m	$emim^+$	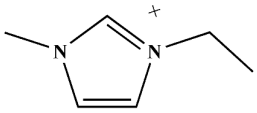
2	1-Butyl-3-methylimidazoliu m	$bmim^+$	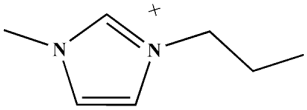
3	N-butyl pyridinium	bpy^+	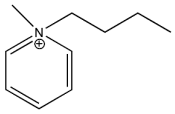
4	N-butyl-N-methyl pyrrolidinium	$bmpyrr^+$	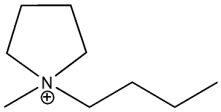

In the ILs-screening process, the performance indicators of extractants must first be determined. For the liquid-liquid extraction, the distribution coefficient (*D*), selectivity (*S*), extractant loss (*SL*), and solvent solubility (*SP*) are often used as extraction indicators. Distribution coefficient (*D*) represents the compositional ratio of solute distribution in two phases at the equilibrium state, which can reflect the extraction ability of the extractant under certain conditions. The greater of the *D* value is, the stronger the extraction ability would be shown. It means that the solute can easily access to the extraction phase and smaller amount of extractant will be cost. The selectivity coefficient (*S*) is the ratio of distribution coefficients between the solute and the solvent, which is similar to the relative volatility in the rectification process. And defined *S* as the difficulty level of separation ability for the extractant. If *S*=1, which indicates that the extractant cannot separate the solute from the solvent.

The larger the selectivity coefficient is, the easier to separate the solute and the solvent. Extractant loss (*SL*) represents the amount of extractant dissolved in the raffinate phase. In the extraction process, the extractant loss is required to be as small as possible in the raffinate phase. Otherwise, the extractant dissolved in the raffinate phase excessively would cause an excessive loss. Solvent solubility (*SP*), which means that the dissolving capacity of compounds to be separated dissolved in the IL extractant. During the extraction process, the greater the *SP* value is, indicating that the greater the solubility of the compounds to be separated dissolved in the extractant. The performance indicators of extractants can be expressed by the following expression.

$$D = \frac{\gamma_{A,B}^{\infty}}{\gamma_{A,S}^{\infty}} \tag{1}$$

$$S = \frac{\gamma_{B,S}^{\infty}}{\gamma_{A,S}^{\infty}} \tag{2}$$

$$SL = \frac{1}{\gamma_{S,B}^{\infty}} \tag{3}$$

$$SP = \frac{1}{\gamma_{A,S}^{\infty}} \tag{4}$$

where $\gamma_{A,B}^{\infty}$ denotes the activity coefficient of component A in component B at infinite dilution, $\gamma_{A,S}^{\infty}$ denotes the activity coefficient of component A in solvent S at infinite dilution, $\gamma_{B,S}^{\infty}$ denotes the activity coefficient of component B in solvent S at infinite dilution, and $\gamma_{S,B}^{\infty}$ denotes the activity coefficient of solvent S in component B at infinite dilution. Hence, in this work, distribution coefficient (*D*), selectivity (*S*), extractant loss (*SL*), and solvent solubility (*SP*) were used to evaluate the ILs for the separation of *N*-compounds.

Meanwhile, for the purpose of decreasing the calculation times, the appropriate IL structures were preliminary selected from 3 common types of cations and 29 kinds of anions by comparing the polarity of the structures based on our previous work. Since the cations of the ILs have similar σ-profile patterns and less influence on separation [9], the cation of 1-ethyl-3-methyl imidazolium ($[emim]^+$), 1-butyl-3-methyl imidazolium ($[emim]^+$), N-butyl pyridinium ($[bpy]^+$) and N-butyl-N-methyl pyrrolidinium ($[bmpyrr^+$), were selected as a model cation. The σ-profiles of the filtered anions

which have strong polarity are presented in Fig. S1.

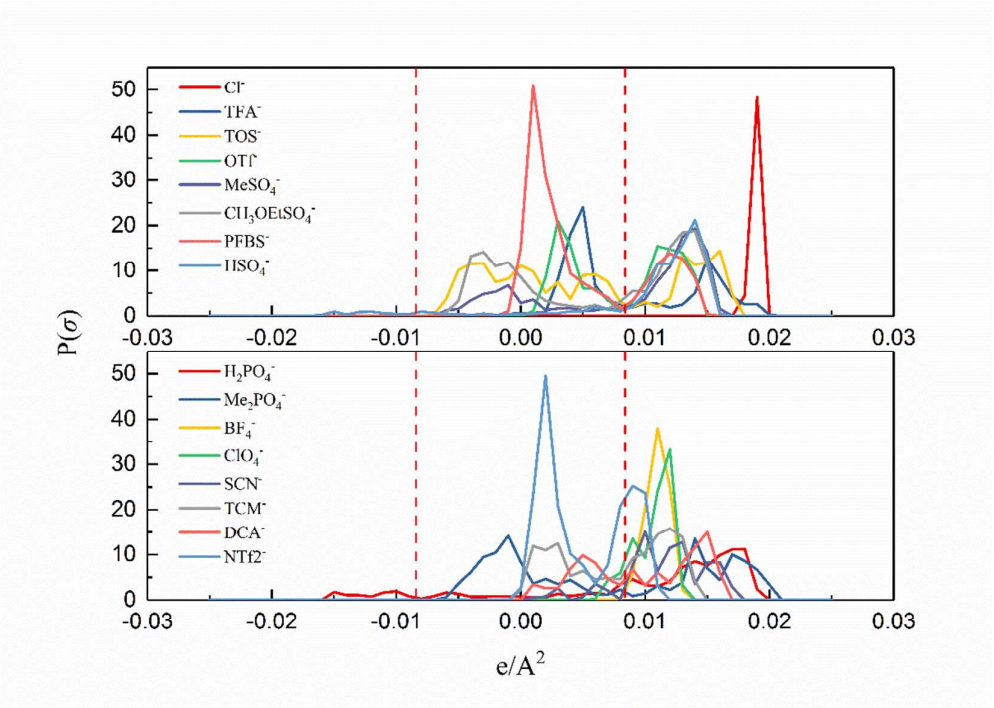

Fig. S1. The σ-profile comparison of the selected anions with strong polarity.

As shown in Fig. S1, two vertical dashed lines represent the cutoff values for the hydrogen bond donor (σ < -0.0084 e/Å^2) and acceptor (σ > 0.0084 e/Å^2). If the profile lies in the left side of -0.0084 e/Å^2, which indicates that the surface segment has the hydrogen bond donor capability, and conversely, it has the hydrogen bond acceptor capability if in the right side of 0.0084 e/Å^2. In addition, the further the peak of the profile is away from the absolute value 0.0084 e/Å^2 on the left or the right, the stronger the hydrogen bond donator or acceptor ability is, respectively.

From Fig. S1, it is shown that the peak of Cl^- is away from the right area, ranging from +0.018 e/Å^2 to +0.020 e/Å^2, which indicates that it has strong hydrogen bond acceptor ability. Similarity, the TFA^-, TOS^-, $H_2PO_4^-$, and $Me_2SO_4^-$ have a relatively strong polarity in the hydrogen bond acceptor area, which have the capability to form a hydrogen bond with neutral *N*-compounds. In addition, based on the above results of σ-profile analysis, 3 types of cations and 16 kinds of anions were further screened for the separation of indole, then 48 kinds of ILs were obtained by random combination

of them. It is no doubt that the experimental verification required a lot of time and cost, in order to guide the extraction and separation of *N*-compounds, the extraction performance of the potential extractants should be determined. Therefore, the calculated distribution coefficient (*D*), selectivity (*S*), extractant loss (*SL*), and solvent solubility (*SP*) of the IL extractants can be obtained using the established method based on the COSMO-SAC model. Then, the IL extractants with excellent extraction performance could be screened quickly with low cost. The specific parameters of the 64 extractants calculated are listed in Table S3 in the following.

Table S3. The calculated results of the distribution coefficients (*D*), selectivity (*S*), extractant cost (*SL*) and the solvent's solubility (*SP*) for ILs to extract indole at 298.15 K

Cations	Anions	*D*	*S*	*SL*	*SP*
$emin^+$					
	Cl^-	74011.26	41573.38	1.79E-11	45886.31
	TFA^-	222.71	1223.35	3.74E-08	138.08
	TOS^-	346.41	935.85	1.12E-07	214.77
	OTf^-	14.54	94.47	9.47E-06	9.01
	$MeSO_4^-$	129.91	557.53	1.77E-07	80.55
	$CH_3OEtSO_4^-$	115.49	361.05	7.46E-07	71.60
	$PFBS^-$	21.84	44.47	1.43E-04	13.54
	HSO_4^-	81.30	513.51	7.23E-09	50.40
	$H_2PO_4^-$	1002.82	3384.84	2.05E-12	621.74
	$Me_2PO_4^-$	3161.28	7500.26	1.20E-09	1959.96
	BF_4^-	9.78	86.59	5.95E-06	6.06
	ClO_4^-	9.61	87.56	6.42E-06	5.96
	SCN^-	126.84	700.08	1.05E-07	78.64
	TCM^-	11.53	68.94	1.99E-05	7.15
	DCA^-	77.01	507.35	2.05E-07	47.75
	NTf_2^-	3.02	4.22	2.49E-02	1.87
$bmim^+$					
	Cl^-	12093.27	29456.25	1.56E-14	7497.72
	TFA^-	109.02	460.14	1.03E-09	67.59
	TOS^-	209.95	541.23	2.64E-09	130.16
	OTf^-	12.02	50.98	1.96E-06	7.46
	$MeSO_4^-$	69.22	332.01	8.47E-09	42.92
	$CH_3OEtSO_4^-$	74.65	226.20	4.37E-08	46.28
	$PFBS^-$	15.46	26.64	2.26E-05	9.58
	HSO_4^-	34.93	295.49	4.46E-10	21.66
	$H_2PO_4^-$	278.33	1728.75	2.10E-14	172.56
	$Me_2PO_4^-$	1302.38	3705.38	7.31E-12	807.47

	BF_4^-	6.14	50.01	2.22E-06	3.81
	ClO_4^-	6.41	49.34	2.32E-06	3.98
	SCN^-	48.09	312.20	5.37E-09	29.82
	TCM^-	9.64	38.04	5.26E-06	5.97
	DCA^-	43.85	244.33	1.15E-08	27.18
	NTf_2^-	2.93	3.15	2.81E-02	1.82
bpy^+					
	Cl^-	19397.04	27750.46	3.42E-10	12025.98
	Ac^-	24799.39	52567.11	6.30E-10	15375.40
	TFA^-	299.95	1102.95	1.16E-06	185.96
	TOS^-	346.43	786.34	2.00E-06	214.78
	OTf^-	20.67	77.45	9.81E-05	12.82
	$MeSO_4^-$	114.16	438.90	2.26E-06	70.78
	$CH_3OEtSO_4^-$	115.29	299.79	8.54E-06	71.48
	$PFBS^-$	27.36	41.85	1.05E-03	16.96
	HSO_4^-	63.33	393.57	9.85E-08	39.27
	$H_2PO_4^-$	622.84	2732.76	5.37E-11	386.16
	$Me_2PO_4^-$	2604.92	6315.86	3.45E-08	1615.02
	BF_4^-	10.29	63.35	4.72E-05	6.38
	ClO_4^-	10.77	64.28	5.42E-05	6.68
	SCN^-	117.70	585.14	1.92E-06	72.97
	TCM^-	16.51	57.49	1.81E-04	10.24
	DCA^-	85.54	394.66	3.74E-06	53.03
	NTf_2^-	3.77	3.81	6.95E-02	2.34
$bmpyrr^+$					
	Cl^-	162287.39	75975.96	5.11E-05	100616.70
	Ac^-	448890.09	395182.26	5.56E-05	278307.75
	TFA^-	2313.00	4072.08	1.00E-03	1434.04
	TOS^-	1422.88	1624.93	1.70E-03	882.17
	OTf^-	70.66	131.72	5.53E-03	43.81
	$MeSO_4^-$	530.60	754.91	1.17E-03	328.97
	$CH_3OEtSO_4^-$	416.21	495.65	2.71E-03	258.05
	$PFBS^-$	75.08	73.95	3.76E-02	46.55
	HSO_4^-	339.54	661.93	4.49E-05	210.51
	$H_2PO_4^-$	4723.40	7078.63	2.10E-07	2928.47
	$Me_2PO_4^-$	18804.09	19643.32	3.34E-04	11658.36
	BF_4^-	39.58	81.78	2.59E-03	24.54
	ClO_4^-	40.81	85.99	2.85E-03	25.30
	SCN^-	806.37	1445.36	9.06E-04	499.94
	TCM^-	53.40	93.99	7.87E-03	33.11
	DCA^-	451.10	838.47	1.35E-03	279.68
	NTf_2^-	5.39	4.39	2.06E-01	3.34

Based on the calculation results of the extraction performance parameters, some

simple and easy synthesized structures can be confirmed. Considering the mutual restriction of separation capability and selectivity, the extractant loss are weighed so as to obtain a more efficiency IL extractants during the separation process. Through the anions of $H_2PO_4^-$, and $Me_2SO_4^-$ also have a wide range in the hydrogen bond donor area and have good extraction performance parameters, but it has been confirmed that these two anions have a good extract ability for basic *N*-compounds, pyridine and quinoline, in previous works [10-12]. Therefore, the ILs with the anions Cl^-, TFA^-, TOS^-, are the promising extractants for separation of neutral *N*-compounds due to their abilities to form hydrogen bonds. Finally, two kinds of imidazolium based ILs with functional anions, [emim][TOS], [emim][TFA], and three imidazolium, pyridinium, and pyrrolidinium cations with the strong polar halogen anion, [bmim][Cl], [bpy][Cl], and[bmpyrr][Cl] were confirmed to extract the neutral *N*-compounds.

Part 2

Table S4. The σ-profile of the selected ILs.

[emim][TOS]		[emim][TFA]		[bmim][Cl]	
-0.025	0.000000	-0.025	0.000000	-0.025	0.000000
-0.024	0.000000	-0.024	0.000000	-0.024	0.000000
-0.023	0.000000	-0.023	0.000000	-0.023	0.000000
-0.022	0.000000	-0.022	0.000000	-0.022	0.000000
-0.021	0.000000	-0.021	0.000000	-0.021	0.000000
-0.020	0.000000	-0.020	0.000000	-0.020	0.000000
-0.019	0.000000	-0.019	0.000000	-0.019	0.000000
-0.018	0.000000	-0.018	0.000000	-0.018	0.000000
-0.017	0.000000	-0.017	0.000000	-0.017	0.000000
-0.016	0.000000	-0.016	0.000000	-0.016	0.000000
-0.015	0.000000	-0.015	0.000000	-0.015	0.000000
-0.014	0.000000	-0.014	0.000000	-0.014	0.000000
-0.013	0.000000	-0.013	0.000000	-0.013	0.000000
-0.012	0.846560	-0.012	0.477820	-0.012	0.719190
-0.011	3.431500	-0.011	3.146720	-0.011	3.702270
-0.010	5.496050	-0.010	5.432260	-0.010	5.955370
-0.009	3.328040	-0.009	3.413510	-0.009	4.174870
-0.008	10.111070	-0.008	7.798720	-0.008	10.296200
-0.007	11.882710	-0.007	12.728460	-0.007	11.453850
-0.006	17.638620	-0.006	13.225070	-0.006	10.619820
-0.005	26.084580	-0.005	14.779420	-0.005	10.264850
-0.004	30.344810	-0.004	17.051580	-0.004	21.204800
-0.003	26.653510	-0.003	15.144780	-0.003	22.444340
-0.002	22.966720	-0.002	16.708900	-0.002	21.235500
-0.001	20.616660	-0.001	14.002880	-0.001	19.807730
0.000	20.608390	0.000	10.177300	0.000	15.001560
0.001	13.599660	0.001	8.108020	0.001	12.978720
0.002	9.822650	0.002	10.972120	0.002	12.583270
0.003	5.576340	0.003	18.348280	0.003	2.076290
0.004	7.090840	0.004	28.615090	0.004	0.740890
0.005	9.460980	0.005	6.894390	0.005	0.062650
0.006	10.727760	0.006	4.883410	0.006	0.433610
0.007	4.965100	0.007	3.625830	0.007	0.112490
0.008	3.894950	0.008	4.795640	0.008	0.639980
0.009	4.745560	0.009	5.945870	0.009	0.945180
0.010	2.516140	0.010	3.109340	0.010	1.425010
0.011	4.200060	0.011	2.090120	0.011	2.405190
0.012	6.093700	0.012	3.763260	0.012	2.020660
0.013	7.744770	0.013	3.689050	0.013	1.039050

0.014	9.806010	0.014	3.559540	0.014	2.463280
0.015	7.161640	0.015	1.032290	0.015	7.888020
0.016	0.528990	0.016	0.000000	0.016	18.408020
0.017	0.000000	0.017	0.000000	0.017	2.871620
0.018	0.000000	0.018	0.000000	0.018	0.000000
0.019	0.000000	0.019	0.000000	0.019	0.000000
0.020	0.000000	0.020	0.000000	0.020	0.000000
0.021	0.000000	0.021	0.000000	0.021	0.000000
0.022	0.000000	0.022	0.000000	0.022	0.000000
0.023	0.000000	0.023	0.000000	0.023	0.000000
0.024	0.000000	0.024	0.000000	0.024	0.000000
0.025	0.000000	0.025	0.000000	0.025	0.000000

[bpy][Cl]		[bmpyrr][Cl]	
-0.025	0.000000	-0.025	0.000000
-0.024	0.000000	-0.024	0.000000
-0.023	0.000000	-0.023	0.000000
-0.022	0.000000	-0.022	0.000000
-0.021	0.000000	-0.021	0.000000
-0.020	0.000000	-0.020	0.000000
-0.019	0.000000	-0.019	0.000000
-0.018	0.000000	-0.018	0.000000
-0.017	0.000000	-0.017	0.000000
-0.016	0.000000	-0.016	0.000000
-0.015	0.000000	-0.015	0.000000
-0.014	0.000000	-0.014	0.000000
-0.013	0.000000	-0.013	0.000000
-0.012	1.242960	-0.012	0.000000
-0.011	3.042570	-0.011	0.000000
-0.010	4.834430	-0.010	0.070650
-0.009	9.411040	-0.009	4.845920
-0.008	7.026190	-0.008	11.493950
-0.007	6.541920	-0.007	11.604550
-0.006	10.559510	-0.006	17.876820
-0.005	11.816740	-0.005	21.135490
-0.004	17.095500	-0.004	21.928640
-0.003	24.958850	-0.003	21.436850
-0.002	29.285640	-0.002	22.959270
-0.001	28.344980	-0.001	20.960390
0.000	18.563700	0.000	11.983200
0.001	9.779200	0.001	8.462940
0.002	10.853040	0.002	8.681580
0.003	3.663680	0.003	3.650860
0.004	0.501620	0.004	0.827750

0.005	0.000000	0.005	0.221280
0.006	0.149450	0.006	0.499160
0.007	0.479620	0.007	0.854000
0.008	0.548580	0.008	0.267510
0.009	0.308400	0.009	0.354030
0.010	0.271330	0.010	0.351410
0.011	1.825900	0.011	2.997230
0.012	3.074540	0.012	4.379670
0.013	2.685970	0.013	0.770740
0.014	1.198040	0.014	0.127420
0.015	2.132620	0.015	2.234620
0.016	7.544990	0.016	6.798480
0.017	16.676550	0.017	19.042540
0.018	1.848920	0.018	1.472160
0.019	0.000000	0.019	0.000000
0.020	0.000000	0.020	0.000000
0.021	0.000000	0.021	0.000000
0.022	0.000000	0.022	0.000000
0.023	0.000000	0.023	0.000000
0.024	0.000000	0.024	0.000000
0.025	0.000000	0.025	0.000000

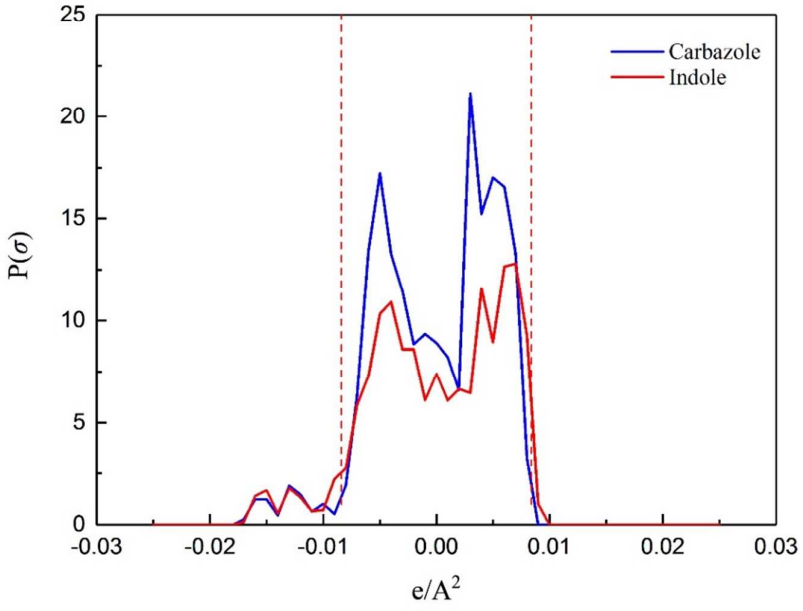

Fig. S2. The σ-profile comparison of indole and carbazole

The screening charge distribution for indole and carbazole are [-0.017, +0.009] e/ Å^2

and [-0.017, +0.008] e/ Å^2, respectively.

Table S5. The results of extraction temperature for *EE* and *D*.

Component	*T*/℃	[emim][TFA]		[emim][TOS]		[bpy][Cl]		[bmpyrr][Cl]	
		EE/%	*D*	*EE*/%	*D*	*EE*/%	*D*	*EE*/%	*D*
Indole	20	87.36	26.33	89.68	28.38	-	-	-	-
	25	87.46	26.34	89.45	27.31	-	-	-	-
	30	-	-	-	-	-	-	86.59	32.28
	35	86.81	24.13	89.48	27.45	-	-	-	-
	40	-	-	-	-	88.57	38.76	90.87	49.79
	45	85.95	21.35	88.56	23.80	-	-	-	-
	50	-	-	-	-	-	-	87.72	38.78
	55	85.03	18.95	87.50	20.58	-	-	-	-
	60	-	-	-		90.12	45.63	85.60	29.72
	80	-	-	-	-	88.21	37.41	80.99	21.30
Carbazole	20	73.68	22.11	73.68	23.32	-	-	-	-
	25	73.57	22.15	73.45	22.42	-	-	-	-
	30	-	-	-	-	-	-	-	-
	35	72.81	20.24	73.48	22.54	-	-	-	-
	40	-	-	-	-	78.57	18.76	65.66	7.71
	45	71.95	17.87	72.56	19.50	-	-	-	-
	50	-	-	-	-	-	-	75.56	14.64
	55	71.03	15.83	71.50	16.82	-	-	-	-
	60	-	-	-	-	80.12	21.63	74.54	14.64
	80	-	-	-	-	78.21	17.41	71.47	12.53

Table S6. The results of mass ratio for *EE* and *D*.

Component	Mass ratio	[emim][TFA]		[emim][TOS]		[bpy][Cl]		[bmpyrr][Cl]	
		EE/%	*D*	*EE*/%	*D*	*EE*/%	*D*	*EE*/%	*D*
Indole	1:10	70.22	23.58	72.21	25.98	81.24	39.06	79.57	38.95
	1:5	85.41	29.27	84.75	27.79	87.26	31.91	86.52	32.10
	1:2	84.64	25.80	87.12	27.49	90.87	27.54	90.48	26.13
	1:1	89.72	27.35	93.83	29.61	96.96	24.62	95.45	21.00
	2:1	93.54	32.00	95.67	35.95	-	-	-	-
Carbazole	1:10	44.65	14.09	56.76	17.28	70.24	15.56	63.3	17.27
	1:5	61.84	18.96	68.30	21.03	76.26	16.06	73.45	14.12
	1:2	70.79	17.93	71.23	20.25	80.27	15.80	83.43	10.07
	1:1	74.15	16.04	80.38	18.92	85.52	14.75	85.31	5.81
	2:1	75.97	14.73	81.22	16.87	90.56	12.59	90.17	3.46

Table S7. The results of extraction time for *EE* and *D*.

Component	*t/min*	[emim][TFA]		[emim][TOS]		[bpy][Cl]		[bmpyrr][Cl]	
		EE/%	*D*	*EE*/%	*D*	*EE*/%	*D*	*EE*/%	*D*
Indole	5	64.76	6.13	67.45	6.31	87.03	33.54	58.51	7.05
	10	76.12	12.23	78.41	12.52	87.56	35.19	83.84	25.93
	30	83.14	23.84	85.35	24.36	88.57	38.76	86.42	31.81
	60	83.23	24.19	85.45	24.75	88.63	38.99	85.94	30.57
	90	82.63	21.96	84.57	22.44	88.43	-	85.34	-
Carbazole	5	59.87	4.77	61.34	5.32	69.03	13.54	70.92	12.19
	10	68.23	10.46	72.30	11.10	77.56	16.19	76.21	16.02
	30	69.25	21.09	79.24	21.75	82.57	18.76	80.96	21.26
	60	69.34	21.44	79.24	22.08	82.63	18.99	80.85	21.11
	90	69.74	19.45	78.46	20.47	81.93	17.96	-	-

Table S8. The results of *N*-initial for *EE* and *D*.

Component	Content/	[emim][TFA]		[emim][TOS]		Content/	[bpy][Cl]		[bmpyrr][Cl]	
	%	*EE*/%	*D*	*EE*/%	*D*	%	*EE*/%	*D*	*EE*/%	*D*
Indole	0.8	86.79	41.25	89.26	42.42	2.5	89.59	49.60	88.75	49.13
	2.4	85.63	35.26	87.82	40.26	4.7	87.52	43.24	86.57	42.77
	6.0	81.03	25.09	83.85	25.96	6.0	85.95	30.97	84.85	30.58
	10.0	79.53	28.19	80.71	28.60	10.2	84.26	22.55	83.25	22.28
						16.1	80.13	17.41	79.99	17.35
Carbazole	0.8	68.05	23.93	73.50	27.48	2.0	81.43	20.67	80.43	19.67
	2.4	64.21	18.41	70.23	23.19	3.64	80.17	17.27	78.87	15.27
	6.0	60.72	15.80	66.98	18.84	7.85	75.79	12.44	74.79	10.44
	10.0	58.39	12.13	63.57	15.08	10.0	71.47	7.22	70.47	5.22

Table S9. The extraction efficiency and distribution coefficient results of different *N*-compounds by [emim][TFA], [emim][TOS] and [bpy][Cl].

Component	[emim][TFA]		[emim][TOS]		[bpy][Cl]	
	EE/%	*D*	*EE*/%	*D*	*EE*/%	*D*
Indole	89.72	27.35	93.83	29.61	96.96	24.62
Carbazole	74.15	16.04	80.38	18.92	85.52	14.75
Pyridine	37.18	0.59	32.48	0.48	14.24	0.17
Quinoline	35.43	0.55	42.24	0.73	28.96	0.41

Table S10. Reusability of [emim][TOS] for neutral *N*-compounds (Indole and carbazole) extraction efficiency (extraction conditions: temperature 25℃, time 30 min, mass ratio 1: 1 for total *N*-content 4.5% model oil).

No. of Cycles	*N*-Extraction Efficiency/ %
1	93.63
2	93.56
3	93.19
4	92.79
5	89.50
6	87.20
7	86.69
8	84.25
9	81.43
10	73.36
11	65.34
12	55.24
13	41.48
14	17.51
15	6.68

References

(1) Lin, S.-T.; Sandler, S. I., A priori phase equilibrium prediction from a segment contribution solvation model. *Ind. Eng. Chem. Res.* **2002,** 41, (5), 899-913.

(2) Li, T.; Yang, Q.; Ding, H.; Li, J.; Peng, C.; Liu, H., Amino Acid Based Ionic Liquids as Additives for the Separation of an Acetonitrile and Water Azeotropic Mixture: COSMO-RS Prediction and Experimental Verification. *Ind. Eng. Chem. Res.* **2015,** 54, (48), 12143-12149.

(3) Varma, N. R.; Ramalingam, A.; Banerjee, T., Experiments, correlations and COSMO-RS predictions for the extraction of benzothiophene from n-hexane using imidazolium-based ionic liquids. *Chem. Eng. J.* **2011,** 166, (1), 30-39.

(4) Lin, S.-T.; Wang, L.-H.; Chen, W.-L.; Lai, P.-K.; Hsieh, C.-M., Prediction of miscibility gaps in water/ether mixtures using COSMO-SAC model. *Fluid Phase Equilib.* **2011,** 310, (1), 19-24.

(5) Hsieh, C.-M.; Sandler, S. I.; Lin, S.-T., Improvements of COSMO-SAC for vapor–liquid and liquid–liquid equilibrium predictions. *Fluid Phase Equilib.* **2010,** 297, (1), 90-97.

(6) Shah, M. R.; Yadav, G. D., Prediction of Liquid–Liquid Equilibria for Biofuel Applications by Quantum Chemical Calculations Using the Cosmo-SAC Method. *Ind. Eng. Chem. Res.* **2011,** 50, (23), 13066-13075.

(7) Zhou, Y.; Xu, D.; Zhang, L.; Ma, Y.; Ma, X.; Gao, J.; Wang, Y., Separation of thioglycolic acid from its aqueous solution by ionic liquids: Ionic liquids selection by the COSMO-SAC model and liquid-liquid phase equilibrium. *J. Chem. Thermodyn.* **2018,** 118, 263-273.

(8) Wang, P.; Xu, D.; Yan, P.; Gao, J.; Zhang, L.; Wang, Y., Separation of azeotrope (ethanol and ethyl methyl carbonate) by different imidazolium-based ionic liquids: Ionic liquids interaction analysis and phase equilibrium measurements. *J. Mol. Liq.* **2018,** 261, 89-95.

(9) Li, J.; Yang, X.; Chen, K.; Zheng, Y.; Peng, C.; Liu, H., Sifting Ionic Liquids as Additives for Separation of Acetonitrile and Water Azeotropic Mixture Using the COSMO-RS Method. *Ind. Eng. Chem. Res.* **2012,** 51, (27), 9376-9385.

(10) Zhang, L.; Xu, D.; Gao, J.; Zhou, S.; Zhao, L.; Zhang, Z., Extraction and mechanism for the separation of neutral N-compounds from coal tar by ionic liquids. *Fuel* **2017,** 194, 27-35.

(11) Zhang, L.; Xu, D.; Gao, J.; Zhang, M.; Xia, Z.; Ma, Y.; Zhou, S., Separation of the mixture pyridine + methylbenzene via several acidic ionic liquids: Phase equilibrium measurement and correlation. *Fluid Phase Equilib.* **2017,** 440, 103-110.

(12) Wang, H.; Xie, C.; Yu, S.; Liu, F., Denitrification of simulated oil by extraction with H2PO4-based ionic liquids. *Chem. Eng. J.* **2014,** 237, 286-290.